Contact Lens and Anterior Eye xxx (xxxx) xxx

Contents lists available at ScienceDirect

Contact Lens and Anterior Eye

journal homepage: www.elsevier.com/locate/clae

Diagnostic age- and sex-adjusted reference intervals of Meibomian gland morphological features

Andrea Novo-Diez [a], Marta Blanco-Vázquez [a], Pablo Arlanzón-Lope [a], Cristina Valencia-Sandonís [a], Margarita Calonge [a,b], María J. González-García [a,b,1,*], Itziar Fernández [a,b,c,1]

[a] IOBA (Institute of Applied Ophthalmobiology), University of Valladolid, Valladolid, Spain
[b] Biomedical Research Networking Center in Bioengineering, Biomaterials and Nanomedicine (CIBER-BBN), Valladolid, Spain
[c] Department of Statistics and Operations Research, University of Valladolid, Valladolid, Spain

ARTICLE INFO

Keywords:
Meibomian glands
Meibography
Reference interval
Dry eye disease

ABSTRACT

Purpose: To establish reference intervals of Meibomian gland (MG) characteristics in healthy participants, and to classify meibography images of evaporative type dry eye disease (DED) subjects according to the determined reference intervals.

Methods: Prospective study including healthy and evaporative type DED subjects. Upper eyelid meibography images were analyzed to evaluate: MG length, minimal distance between endpoints, tortuosity, width, MG shortening area, deviation from a vertical orientation, number of linear segments, MG global area, and number of MGs. Reference intervals for MG characteristics were determined using generalized additive models for location, scale, and shape (GAMLSS). Participants with evaporative type DED were classified as normal or non-normal based on the reference intervals. Clinical features were compared between groups using Student's *t* test or Mann–Whitney *U* test.

Results: Participants were 156 healthy individuals (50.6 % males; mean age 44 years) and 39 individuals with evaporative type DED (74.4 % women; mean age 62 years). MG length, minimal distance between endpoints, tortuosity, and width, depended on age but not on sex. MG shortening area depended on age and sex. Neither age nor sex affected the deviation from a vertical orientation, number of linear segments, MG global area, and number of MGs. Furthermore, 66.7 % of the participants in the evaporative type DED group were classified as normal (all the MG characteristics fell within the corresponding reference intervals). A significantly higher value was observed in the non-normal group in OSDI ($P = 0.034$) and meibum expressibility ($P = 0.041$, indicative of poor expressibility).

Conclusions: Reference intervals values may be useful in classifying meibography images as normal or non-normal, thus aiding in the objective diagnosis of morphological alterations of MGs.

1. Introduction

The worldwide prevalence of dry eye disease (DED) is 29.5 %, higher in women (28.1 %) than men (24.9 %), and increases with age [1], with evaporative type DED caused by meibomian gland dysfunction (MGD) being the most common [2].

Meibomian glands (MGs) are sebaceous glands located in the upper and lower eyelids [3]. They deliver meibum to the tear film, stabilizing it and preventing evaporation [4]. Alterations in meibum composition can lead to MGD [5], and the proper functioning of the MG depends to a large extent on its morphology [6]. Meibography is the most used method for observing MG morphology. Habitually, these images have been evaluated using subjective scales to quantify MG loss [7]. However, the use of automatic software tools enables quantifying new characteristics of MG morphology, such as length, width, and tortuosity [8–13].

MG loss increases with aging in healthy subjects [8,14–16]. However, the age at which this loss begins remains unclear. Some studies suggest it starts between 20 and 25 years of age [17], whereas others

* Corresponding author at: IOBA, Universidad de Valladolid Campus Universitario Miguel Delibes, Paseo de Belén 17, 47011, Valladolid, Spain.
E-mail address: mariajesus.gonzalez.garcia@uva.es (M.J. González-García).

[1] Dr. María J. González-García and Itziar Fernández contributed equally as co-last authors.

https://doi.org/10.1016/j.clae.2025.102447
Received 23 December 2024; Received in revised form 18 May 2025; Accepted 20 May 2025

place it during adolescence [18,19]. Analyzing changes in the MG associated with factors such as age and sex could improve MGD diagnosis.

The conventional approach for evaluating diagnostic efficacy involves comparing differences between groups of patients and controls to confirm a diagnosis [20–23]. However, a more general strategy involves building reference intervals [24,25]. Reference intervals are statistical ranges that define the expected values of a parameter in a healthy population, typically encompassing the central 95 % of the distribution. These intervals are fundamental in clinical practice as they provide a standardized framework to evaluate whether a test result fall within normal limits or suggest an underlying abnormality. This approach simplifies the application in clinical scenarios, where the aim is to assess a single patient rather than to analyze population differences. In the field of visual sciences, a similar approximation has been used in the area of myopia management, generating the percentile curves of axial length as a function of age [26]. The generalized additive models for location, scale, and shape (GAMLSS) methodology provides a robust and flexible framework for accurately estimating reference intervals [27]. GAMLSS are a versatile statistical methodology capable of modelling complex relationships in data, such as non-linear patterns (when relationships between two variables cannot be described by a straight line), heteroscedasticity (when the variance of the errors is not constant over all observations made), and distributional asymmetries (when the data distribution around a central point is imbalanced).

In this study, the aim was to use GAMLSS models with a large sample size of participants without ocular pathology to accurately describe various MG morphological characteristics derived from upper eyelid meibography images, verify the influence of age and sex as determining factors, and establish age- and sex-adjusted reference intervals. These reference intervals could serve as diagnostic aids to identify abnormalities in MG morphology and classify participants with evaporative type DED based on MG morphology.

2. Methods

The East Valladolid Health Area Ethics Committee (Valladolid, Spain) approved this prospective study, which was conducted in compliance with the tenets of the Declaration of Helsinki. Written informed consent was obtained from all participants before enrollment.

The overall methodology is explained in Fig. 1. Two samples were initially recruited: a sample of healthy individuals (healthy group) and a sample of patients with evaporative type DED (evaporative-type DED group). The first step was to define the MG morphology in the healthy group. The second step was to select the best GAMLSS model. The third step was to calculate the reference intervals as a function of age and sex for each MG characteristic. The fourth step was to apply the established reference intervals to classify the MG morphology of the evaporative type DED group as normal and non-normal: meibography images of the evaporative type DED group were analysed to extract MG features values; then participants were classified as normal if all values fell within the corresponding reference intervals, and as non-normal if at least one value lay outside these intervals. Fifth and final step was to compare the clinical values between the normal and non-normal group.

2.1. Study samples

This study included volunteers aged 16–76 years. Inclusion criteria were having no preexisting eye disease. Exclusion criteria were any acute or chronic ocular disease, systemic disease, use of medication that could affect the ocular surface, history of contact lens wear and ocular surface surgery, use of topical ocular medication in the previous 3 months, pregnancy, and breastfeeding.

To assess the utility of the age- and sex-related reference intervals, they were applied to classify participants from an external sample. Inclusion criteria was having evaporative type DED due to MGD. Exclusion criteria were punctal occlusion in the previous 3 months, contact lens wear in the previous week, and use of topical ocular medication in the previous 24 h. DED was defined as having two or more of the following test results altered: ocular surface disease index (OSDI) $\geq$13 [28], tear fluorescein break up time (TFBUT) $\leq$7 s [29], fluorescein corneal staining $\geq$1 in the Oxford scheme [30], lissamine green staining $\geq$1 in the Oxford scheme [30], and Schirmer's test values without anesthesia $\leq$5 mm in 5 min [31]. MGD presence was defined by meibum expressibility and quality $\geq$2 based on the Bron and Shimazaki scales [32,33].

2.2. Clinical evaluation

Ocular symptoms were evaluated using the OSDI questionnaire, scored from 0 to 100, considering as symptomatic a value $\geq$13 [28]. Sodium fluorescein strips (I-DEW FLO; Entod Research Cell, Ltd. London, UK) were wetted with sodium chloride, and fluorescein break up time (TFBUT) was measured under cobalt blue light and the Wratten #12 yellow filters (Eastman Kodak, Rochester, NY, USA). TFBUT was defined as the time between the last of three blinks and the appearance of the first dry spot. The procedure was repeated thrice, and the mean values were recorded [34]. Corneal fluorescein staining was graded from 0 (no staining) to 5 (severe staining) using the Oxford scheme [30]. Marx's line displacement was evaluated in both eyelids from 0 (no displacement) to 9 (high displacement) using Yamaguchi's scale [35]. Lissamine Green strips (I-DEW Green; Entod Research Cell, UK Ltd. London, UK) were wetted and used to evaluate conjunctival staining from 0 (no staining) to 5 (high staining) using the Oxford scheme [30]. MG function was evaluated by grading meibum expressibility (Shimazaki scale) and quality (Bron scale) from 0 (easy expressibility, clear quality) to 3 (no expressibility, inspissated quality) [32,33]. Infrared meibography was performed on the upper eyelid using the Easy Tear View+ (EASYTEAR S.R.L., Trento, Italy). Finally, the Schirmer's test was performed without anesthesia. Schirmer's strips (I-DEW Tearstrips; Entod Research Cell Ltd., London, UK) were applied to the inferior fornix, and the wet length was measured after 5 min with the eyes closed. Both eyes were evaluated. For data analysis, one eye was randomly selected to avoid bias.

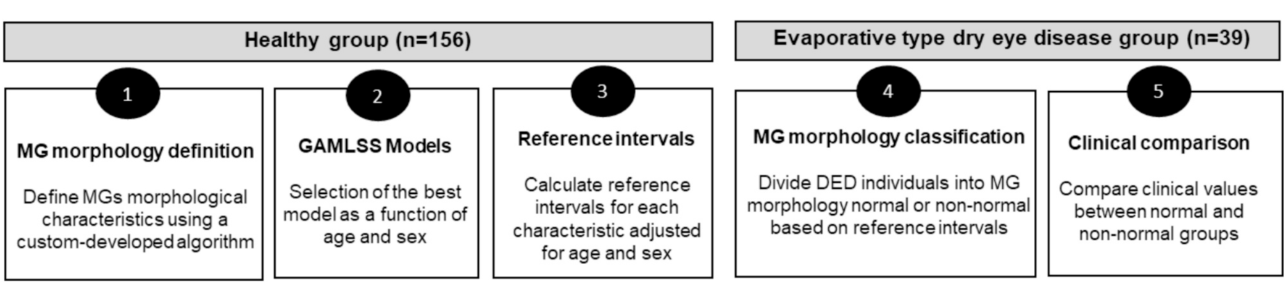

Fig. 1. Schematic presentation of the methodology of the study. MG: Meibomian gland. DED: dry eye disease.

2.3. MG feature extraction

Meibography images were analyzed using a custom-developed algorithm implemented in the R statistical software and developed by co-author IF. Using this algorithm, each image was processed, skeletonized and finally, each MG was divided into linear segments based on changes in direction using a piecewise regression model (see Supplementary Material, Section 1. Image analysis process, eFig. S.1). Based on these piecewise regression models, 6 individual MG metrics were quantified: length, minimal distance between endpoints, deviation from a vertical orientation, number of linear segments, tortuosity, and width. For each image, the individual MG metrics were summarized using the median value of all analyzed glands in the same image. In addition, 3 global metrics were included: the MG global area, the MG shortening area, and the number of MGs (Table 1).

2.4. Reference intervals determination

Reference intervals were calculated for each MG characteristic to be used as a diagnostic rule when classifying a value as normal or non-normal. For example, assuming that the reference interval of MG area for 50-year-old individuals is between 10 % and 20 %, a subject with 5 % would be classified as having an altered MG area (outside the normal range), while a patient with 15 % would be classified as having a normal MG area.

GAMLSS models were used to estimate the 5th and 95th percentile curves for each of the variables related to MG morphology, considering the possible influence of age and sex of the subjects, which results into the 90 % reference intervals. The GAMLSS package [27], R version 4.2.1 [36], was used to fit one of these models to each of the variables related to MG morphology. Model validation and diagnosis were verified by evaluating the randomized/normalized quantile residuals [37]. Additionally, a worm plot was used to identify possible ranges of explanatory variables where the model did not adequately fit. Fig. 2 summarizes the fitting of the GAMLSS models and the estimation of the corresponding percentile values. More details on the analysis can be found in the Supplementary Material (Section 2: Reference Interval Determination, eTable S.1–3 and eFig. S.2).

2.5. Data analysis

Sex, a categorical variable, is expressed as a percentage. Quantitative variables are expressed as means and 95 % confidence intervals (CIs) for the mean, minimum, and maximum. Ordinal variables are expressed as median, interquartile range (IQR), minimum, and maximum. The normal distribution assumption was verified using the Shapiro–Wilk test for small sample sizes (<50 participants) and the Kolmogorov–Smirnov test for larger samples.

Using the age- and sex-related reference intervals estimated with GAMLSS models, participants from the evaporative type DED group were classified as non-normal when the observed value of at least one of the characteristics related to MG morphology was outside the corresponding reference interval. Clinical features were compared between the normal and non-normal groups. Student's *t*-test for two independent samples was used when the hypotheses of normality and homogeneity of variance were met. The homogeneity of the variance hypothesis was tested using Levene's test. When this could not be assumed, a robust Welch test was used to compare the means. If the normality hypothesis could not be assumed, a nonparametric alternative, the Mann–Whitney *U* test, was used.

3. Results

3.1. Sample description

Overall, 156 participants were included in the healthy sample. The mean age was 44 years (95 % CI: 41–46), and approximately half were men (n = 79; 50.6 %). In the evaporative type DED sample, 39 participants were included (74.4 % women; mean age 62 [95 % CI: 58–65] years; range 45–89). More information has been included in the Supplementary Material, section 4. Supplementary Results, 3.1 Demographic distribution, eTable S.4–5, that shows the age and sex distributions of the participants. Table 2 presents the results of the clinical evaluation, and Table 3 presents the mean values of the MG morphological characteristics for both samples.

3.2. Reference intervals for MG morphology

Model selection involved selecting the distribution and identifying relevant explanatory factors (see Supplementary Material, section 3. Suplemmentary Results, 3.2 Distributions selected, eTable S.6–9 lists the best GAMLSS models for each morphological characteristic of MGs).

Fig. 3 represents the age- and sex- adjusted reference curves for each morphological characteristic of the MG where age and/or sex had an effect.

Regarding the individual measurements, age had an influence in length (mean = 2.2 mm, 95 %CI [2.1–2.2 mm]) and the minimal distance between endpoints (mean = 2.1, 95 %CI [1.9–2.1 mm]), increasing between 25 and 50 years of age. Neither age nor sex had any effect on deviation from a vertical orientation (mean = 0.4, 95 %CI [0.3–0.4], reference interval: 0.3–0.5), and number of linear segments (mean = 6.1, 95 %CI [5.8–6.4], reference interval: 3–9). Finally, age had an influence in tortuosity (mean = 0.3, 95 %CI [0.3–0.3]) and width (mean = 0.3 mm, 95 %CI [0.3–0.4 mm]), increasing with age and narrowed between 45 and 60 years of age. For width, the reference interval remained constant between 20 and 55 years of age and narrowed thereafter.

Regarding the global measures, neither age nor sex had any effect on the MG global area, remaining constant (mean = 14 %, 95 %CI [14–15 %], reference interval: 8–20 %). Age and sex had an influence in MG shortening area (mean = 63 %, 95 %CI [62–64 %]), increasing with age in men and women, although higher values were observed in men. Neither age nor sex had any effect on the number of MGs (mean = 16.1, 95 %CI [15.3–16.8], reference interval: 8–27).

Residual analysis of each of the final fitted models was performed. During the diagnostic stage, none of the features exhibited inadequacy in the final fitted model (see Supplementary Material, section 4. Residual analysis, eTable S.11-12, eFig. S.3.20).

3.3. Diagnostic utility of estimated RIs

According to the reference intervals classification, 66.7 % (95 % CI: 49.7–80.4) of the participants with evaporative type DED were classified as normal (normal) and 33.3 % (95 % CI: 19.6–50.3) as non-normal (non-normal). The MG characteristics altered can be found in the Supplementary Material, Section 3. Supplementary Results, 3.3 Reference intervals applied for the evaporative type dry eye group, eTable S.10. Once this classification was established, the clinical variables of the normal group were compared with those of the non-normal group. A significantly higher value was observed in the non-normal group in OSDI and meibum expressibility (indicative of poor expressibility), whereas meibum quality was on the edge of significance. No significant differences were observed among the other variables analyzed (Table 4).

4. Discussion

In this study, age- and sex-adjusted reference intervals for various morphological characteristics of MGs in the upper eyelid were established and applied to classify participants with evaporative type DED. In healthy participants, MG length, minimal distance between endpoints, tortuosity, and width depended on age, whereas MG shortening area depended on age and sex. However, deviation from a vertical

Table 1
Measures obtained from the MG feature extraction.

Measure	Type	Description	Units	Graphical description
MG Length	Individual	Cumulative pixel-wise length across all linear segments that formed the gland within the skeletonized image	Pixels converted to mm	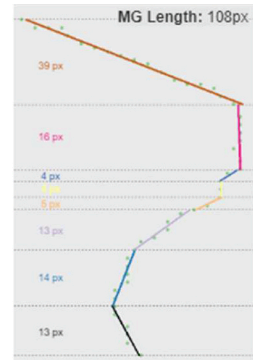
Minimal distance between endpoints	Individual	Euclidean distance between its endpoints	Pixels converted to mm	
Deviation from a vertical orientation	Individual	Determined by measuring the MG inclination degree with respect to the vertical reference lines	Index (from 0 as minimum to 1 as maximum)	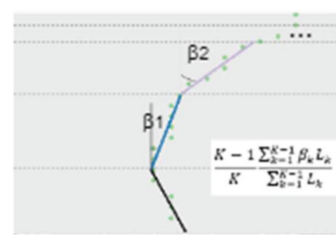
Number of linear segments	Individual	Each MG is divided into linear segments according to their changes of direction	Units (0-∞)	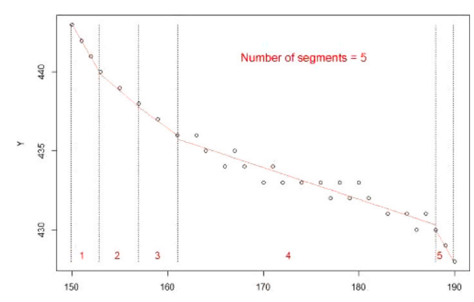

(continued on next page)

Table 1 (*continued*)

Measure	Type	Description	Units	Graphical description
Tortuosity	Individual	Assessed by evaluating the slope changes between consecutive straight-line linear segments, and summarized as an index obtained by summing the product of each angle and its corresponding linear segment length divided by the total linear segment length	Index (from 0 as minimum to 1 as maximum)	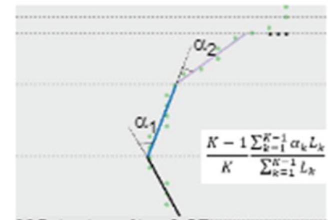
Width	Individual	Average of the number of pixels in the horizontal orientation in the image before skeletonization	Pixels converted to mm	
MG global area	Global	Proportion of the eyelid area covered by MGs in the pre-skeletonized image	Percentage (0–100)	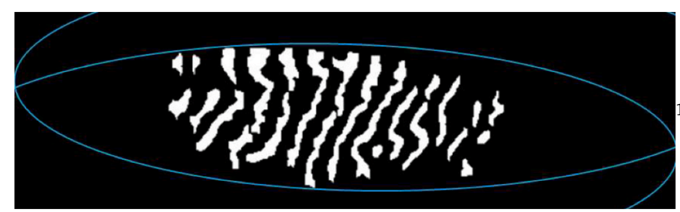 18%
MG shortening area	Global	Proportion of the MG area considering only the half closest to the free eyelid margin	Percentage (0–100)	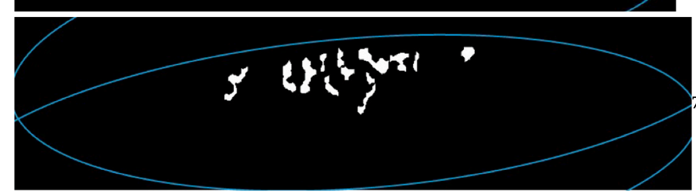 76% of the global MG area

(*continued on next page*)

Table 1 (*continued*)

Measure	Type	Description	Units	Graphical description
Number of MGs	Global	Number of MGs in the skeletonized image	Units (0-∞)	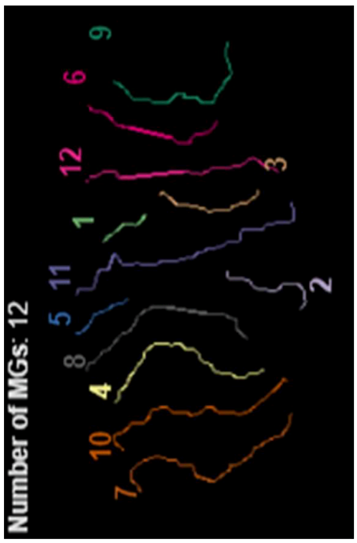

MG: Meibomian gland; mm: millimeters.

orientation, the number of linear segments, the MG global area, and the number of MGs remained constant. By applying these reference intervals, 33.3 % of the participants with evaporative type DED had an altered MG morphology compared to the healthy group of reference, and these participants had more severe ocular symptoms and worse MG function.

This study proposed two novelties: evaluating new variables related to the morphology of MGs and establishing an age and sex-adjusted reference intervals for the described variables in meibography images, configuring a diagnostic rule of what is defined as normal in healthy individuals. The most important advantage of using reference intervals is that although they are established on the basis of a group of individuals, it is not necessary to have a group to make decisions about an individual case. A single individual's value outside the reference interval can already help in its diagnosis, without requiring a direct comparison with a group. In clinical practice, cut-off points are commonly used to determine whether a test result is normal or abnormal. This approach is useful when there is a clear relationship between the variable of interest and the disease, but has limitations, such as the possibility of generating false positives or false negatives if the threshold is not well defined due to significant biological variability, or the continuous nature of the variable. The advantage of reference intervals over cut-off points is that cut-off points do not consider anything other than the variable of interest, whereas reference intervals allow modelling of the values of the variable taking into account other characteristics that may influence it, such as age and sex, resulting in a more personalised approach. Reference intervals also allow to assess whether an individual is within the expected range according to his or her specific characteristics as they take into account the natural variability that exists in the variables of interest.

Age had an effect on MG length as both mean values and IRs increased between the ages of 20 and 60. The mean values obtained in the present study are consistent with those published for an age range of 40–45 years, which were also obtained automatically [38]. Another study found a higher value and negative correlation with age [8]. These results may be attributed to a bias introduced by the selection of the five central MGs, as MGs are longer in the center of the eyelid. In contrast, in the present study, the length of all the MGs were quantified, except for small regions of the temporal and nasal areas, which were not considered owing to lower visibility.

Similar behavior was observed in the minimal distance between endpoints. Furthermore, it has been observed that the mean values of minimal distance between the endpoints of the MGs are similar to those of MG length, and the path of reference intervals over age is also similar. The ratio of the length to minimal distance between endpoints has previously been used as an index of tortuosity [12,13]. However, assessing tortuosity using this ratio may not be a good indicator, as tortuosity refers to a change in direction along the path of a straight line. The ratio of the MG length to minimal distance between endpoints of the MG could be more useful when circular-type MGs predominate but is similar to the MG length of the gland in other cases, an issue that does not affect in the proposed concept of tortuosity.

Age had an effect on tortuosity since although the mean value remained almost constant, the reference intervals narrowed between the ages of 45 and 60 years, indicating lower variability in that age range, but sex did not. A tortuosity mean value of 0.3 and reference interval values between 0.2 and 0.4 was found. However, these results are not comparable to those of previous studies because the tortuosity definition is different, along with differences in the quantification method. One study found a mean of 2 MGs distorted per eyelid [39], another study found a mean of 0.11 of tortuosity in a 0–2 scale [10], and two studies found a mean of 0.2 [12] and 1.68 [13] using the MG length/Euclidean distance ratio. In other studies where tortuosity has been analyzed, the relationship between tortuosity and age or sex has not been studied [12,13,39].

Age also had an effect on the width because although the mean value

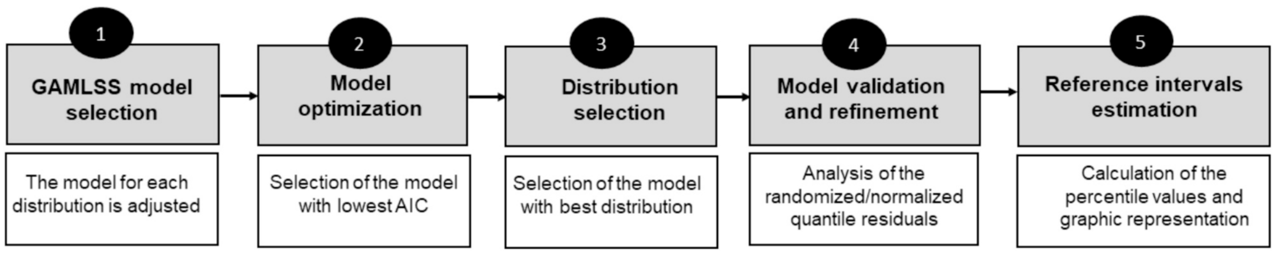

Fig. 2. Summary of the estimation of the GAMLSS models and the calculation of the percentile values. GAMLSS, using generalized additive models for location, scale, and shape; AIC: Akaike information criterion.

remained almost constant, the reference intervals narrowed from the age of 60 onwards, indicating less variability. The mean values obtained are similar to those reported in a previous study [39].

No influence of age or sex was observed in the MG global area. The mean value was 14 % and the reference interval varies from 8 to 20 %. These results contrast with what has been published so far, since a relationship between the increase in the degree of MG loss and age has been described in healthy individuals [15]. These differences may be due to the method of evaluation of the area of interest, obtaining different values depending on whether the area of loss, the area occupied by the MG, and whether the interglandular space is included. In the present study, the MG global area was defined as the ratio between the eyelid area and the area occupied by the MGs. However, with regard to the effect of sex, the results are in line with those of Chen *et al.* [40] who found no differences between men and women in the area of loss in a sample of individuals without DED. The results of this study indicate that in people without ocular surface pathology, age has no effect on the area occupied by MGs.

With respect to MG shortening area, it was observed that both mean values and reference intervals increased with age and were higher in men than in women. The MG shortening area values indicated that if the eyelid is divided into two equal halves, the upper half being the one closest to the palpebral margin, 63 % of the area occupied by the MGs is in that upper half. Therefore, a value greater than 50 % indicates a shortening of the MGs. This may indicate MG shortening area more accurately than length does, as percentage is a relative variable that considers the total eyelid area whereas length is an absolute measure. In fact, studies quantifying the percentage loss with Image J software actually measure the area to which the MGs reach, so it would perhaps be more appropriate to speak of MG shortening area rather than degree of loss, as a subject with all MGs shortened would have the same percentage as a subject with MG loss in a particular area of the eyelid, such as the nasal or temporal area. This measurement makes it possible to distinguish whether the MGs have shortened or whether they have been lost only in one sector of the eyelid. This parameter may have substantial clinical utility. Age and sex influenced this variable; therefore, considering these two demographic variables when assessing whether the shortening area of the MGs is within or outside the normal range is necessary.

Finally, neither age nor sex had an effect on the number of MGs. A wide reference interval (from 8 to 27) was observed in comparison with other studies although the mean value (mean = 16.1) was similar [13,38]. In the present study, the degree of MG loss was not an inclusion

Table 2
Clinical evaluation results of healthy participants and patients with evaporative type DED.

Test	Sample	Mean (95 % CI)	Range	*P* value
OSDI (0–100)	Healthy	3.6 (3.0–4.1)	0–12.5	<0.001
	Evaporative DED	32.8 (26.4–39.1)	13–82.5	
TFBUT (seconds)	Healthy	9.8 (9.5–10.9)	2.3–38	<0.001
	Evaporative DED	3.3 (2.9–3.7)	1.3–7	
Marx Line (0–18)	Healthy	5.3 (4.7–5.8)	0–15	<0.001
	Evaporative DED	9.3 (8.1–10.4)	0–15	
Conjunctival staining (0–5)	Healthy	0.5 (0.3–0.6)	0–4	<0.001
	Evaporative DED	2.3 (1.9–2.8)	0–5	
Schirmer's test (mm)	Healthy	17.4 (15.3–19.5)	1–35	0.006
	Evaporative DED	11.7 (8.7–14.7)	0–35	
Test	**Sample**	**Median [IQR]**	**Range**	***P* value**
Corneal staining (0–5)	Healthy	0 [0]	0–1	<0.001
	Evaporative DED	1 [1]	0–4	
Meibum expressibility (0–3)	Healthy	0 [1]	0–2	<0.001
	Evaporative DED	2 [1]	1–3	
Meibum quality (0–3)	Healthy	1 [1]	0–2	<0.001
	Evaporative DED	2 [1]	1–3	

CI, confidence interval; DED, dry eye disease; IQR, interquartile range; OSDI, ocular surface disease index; TFBUT, tear film break-up time.

Table 3
Morphological characteristics of Meibomian glands of healthy participants and those with evaporative type DED.

Variable	Sample	Mean (95 % CI)	Range	*P* value
MG Length (mm)	Healthy	2.1 (2.1–2.3)	0.8–4.6	***0.030***
	Evaporative DED	1.9 (1.7–2.2)	0.7–4.0	
Minimal distance between endpoints (mm)	Healthy	2.0 (1.9–2.1)	0.8–4.4	0.053
	Evaporative DED	1.9 (1.6–2.1)	0.7–4.1	
Deviation from a vertical orientation (0–1)	Healthy	0.4 (0.4–0.4)	0.3–0.5	0.405
	Evaporative DED	0.4 (0.4–0.4)	0.3–0.5	
Number of linear segments	Healthy	6.1 (5.8–6.4)	2.2–13.4	***0.025***
	Evaporative DED	5.4 (4.8–5.9)	2.3–9.6	
Tortuosity (0–1)	Healthy	0.3 (0.3–0.3)	0.1–0.4	0.936
	Evaporative DED	0.3 (0.3–0.31)	0.1–0.4	
Width (mm)	Healthy	0.3 (0.3–0.4)	0.2–0.5	0.457
	Evaporative DED	0.4 (0.3–0.4)	0.1–0.2	
MG global area (0–100)	Healthy	0.1 (0.1–0.1)	0.1–0.2	0.147
	Evaporative DED	13.4 (11.7–15.0)	4.4–24.1	
MG shortening area (0–100)	Healthy	0.6 (0.6–0.6)	0.5–0.9	0.432
	Evaporative DED	62.2 (60.2–64.1)	43.4–74.8	
Number of MGs	Healthy	16.1 (15.3–16.8)	7–32	0.655
	Evaporative DED	15.1 (13.3–16.8)	3–24	

CI, confidence interval; DED, dry eye disease; MG, Meibomian gland.

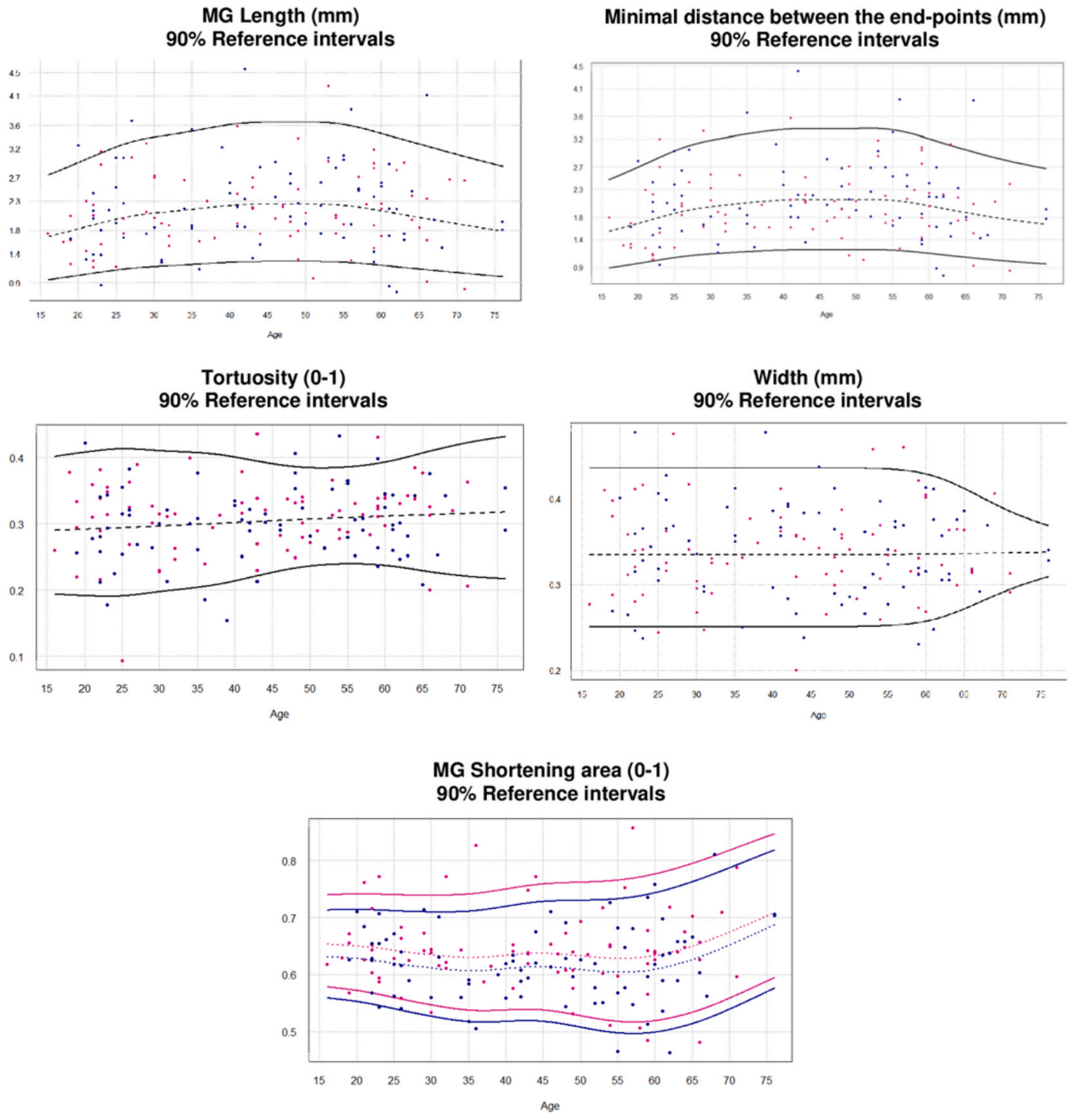

Fig. 3. 90 % Reference intervals based on Meibomian gland (MG) morphological characteristics depending on age and sex. The black lines represent the 90 % reference intervals, and the dotted line represents the median. Blue dots and lines represent values for women, whereas pink dots represent values for men. (For interpretation of the references to colour in this figure legend, the reader is referred to the web version of this article.)

Table 4
Clinical results of the normal and non-normal groups in DED participants.

Test	Group	Mean (95 % CI)	Range	*P* value
OSDI (0–100)	normal	29.1 (21.2–36.9)	22.2–77.5	0.034
	non-normal	40.1 (28.9–51.4)	15.5–82.5	
TFBUT (seconds)	normal	3.3 (2.8–3.8)	1.3–6	0.787
	non-normal	3.3 (2.3–4.2)	1.7–7	
Marx Line (0–18)	normal	9.1 (7.7–10.5)	2–15	0.725
	non-normal	9.5 (7.3–11.6)	3–14	
Conjunctival staining (0–5)	normal	2.5 (2–3)	1–5	0.391
	non-normal	2.1(1–3)	0–5	
Schirmer's test (mm)	normal	11.2 (7.4–15.1)	0–35	0.540
	non-normal	12.8 (7.3–18.3)	1–30	
Test	**Group**	**Median [IQR]**	**Range**	***P* value**
Corneal staining (0–5)	normal	1 [1]	0–2	0.241
	non-normal	1 [0]	0–3	
Meibum expressibility (0–3)	normal	2 [1]	1–2	0.041
	non-normal	2 [0]	1–3	
Meibum quality (0–3)	normal	2 [1]	1–3	0.052
	non-normal	2 [0]	1–3	

CI, confidence interval; TFBUT, tear fluorescein break-up time; IQR: interquartile range; OSDI, ocular surface disease index.

criterion; therefore, the variability in the number of MGs may be because of the different degrees of MG loss in the included participants. This variability could explain the discrepancies with other studies owing to the inclusion of participants with different degrees of MG loss [13,38].

The results found in the present study are important for two reasons. On the one hand, they show a variability in the morphology of MGs in healthy individuals, i.e. there is not a single reference value considered "normal", but rather an interval of values considered "normal", which cover the reality of the population and could be used as a reference for normality. On the other hand, these reference intervals vary depending on factors such as age or sex. Therefore, when assessing an individual, it should be classified as pathological if the values are outside the reference interval according to age and sex, by consulting the curves and percentile tables proposed in this study.

With the parameters used and the calculated reference intervals, 66 % of the participants with evaporative type DED had an upper eyelid MG morphology within normal limits. The MG global area was the most altered characteristic, whereas the MG shortening area was the least altered. Although all the patients included had evaporative type DED, it can also be observed that they had a medium-moderate degree (Table 2). This can be explained by the fact that alterations in MG function occur before alterations in its morphology [3,41–43], even alterations in MG expressibility have been observed even with an unaltered morphology [44]. Some authors argue that meibum viscosity increases first [45,46], leading to the obstruction of orifices and [47,48] causing MG atrophy and loss [15].

The findings of the present study align with this theory, as participants with evaporative type DED had altered MG function relative to that of healthy participants, but MG morphology was within the reference intervals in 66 % of them. These findings reinforce prior evidence that MGD involves both morphological and functional alterations. Importantly, they further demonstrate that altered MG morphology does not necessarily correlate with impaired function, underscoring that altered MG morphology alone is insufficient for diagnosing MGD.

The non-normal group had a higher degree of symptoms and worse expressibility of MG secretion, indicating that alterations in MG morphology occur in severe cases of evaporative type DED and, therefore, could be useful for detecting such cases but not for mild and moderate cases. These results align with those of other studies, which state that the degree of MG loss is related to the severity of DED [39,49–51]. Finally, no significant differences were observed in the remaining clinical tests, which could be attributed to the lack of correlation between the signs and symptoms of DED [50,52].

The results of this study suggest that meibography should not be used in isolation for evaporative type DED diagnosis. Along with meibography and the proposed reference intervals, other tests such as symptomatology or MG function should be performed. The alterations in MG morphology of the upper eyelid had a greater effect on symptoms than on signs, indicating that, in two participants with evaporative type DED of equal severity, when assessing only ocular signs, the subjective severity may differ. Thus, assessing MG morphology could provide more information, indicating whether it is inside or outside the reference interval, and help detect cases with worse MG function and a higher degree of symptoms when ocular signs are similar.

It is important to emphasize that reference intervals identify structural deviations relative to healthy norms, but are not intended as diagnostic tools per se. As such, the fact that a large proportion of patients with evaporative DED were classified as morphologically normal does not imply misclassification, but rather reflects the variability in disease presentation. Functional impairment often precedes detectable structural changes in MGs, and the findings of this study align with this interpretation. Therefore, reference intervals may be particularly useful in identifying more advanced cases or in supplementing functional assessments in a multimodal diagnostic approach.

This study has some limitations. Only images of the upper eyelid were evaluated because of the difficulty in obtaining quality meibography scans of the lower eyelid; for this reason, most of the published studies are focused on the upper eyelid [8,11–13,22,38,39,53]. Moreover, the software developed depends on the instrument used to capture the images (Easy Tear View+), because different parameters were adjusted to process the images obtained from this instrument. This dependence exists in the early stages of the analysis, as the MG modeling and quantification stages are valid for any instrument used, and the group is working to adapt it to other instruments. Another limitation lies in the order of clinical testing, as meibography imaging was performed after meibum expressibility assessment. Although this sequence followed standard clinical protocols and published studies at the time of recruitment [8,9,15,38], and all images were acquired during clinical visits under consistent conditions, recent research [54] suggest that therapeutic gland expression may transiently alter MG morphology, including reduced brightness and length in infrared images, and that MG structure may exhibit temporal variability throughout the day [55]. Although the expression of MG in this study is performed only with diagnostic purposes, therefore the conditions in terms of time and pressure may be different, future studies should consider the possible influence of test order and time of image acquisition when designing protocols involving morphological assessments of the MG.

5. Conclusions

This study characterizes upper eyelid MG the morphology in healthy participants and establishes reference intervals across a broad age range. It also introduces new objectively measured parameters, accounting for the influence of age and sex. These values are useful for classifying meibography images as normal or non-normal, thus helping to objectively diagnose MG morphological alterations. Alterations in MG morphology may contribute to detecting cases with worse MG function and a higher degree of symptom severity when the ocular signs are similar in patients with evaporative type DED.

Funding and role of funder

AN-D was supported by the Junta de Castilla y León predoctoral program "Convocatoria 2018 ayudas destinadas a financiar la contratación predoctoral de personal investigador, cofinanciadas por el Fondo Social Europeo," an Erasmus + training grant course 2019/2020, a mobility grant from the University of Valladolid "Movilidad doctorandos Uva 2019," and a research grant (short-term grant of the German Academic Exchange Service, course 2022).

Declaration of competing interest

The authors declare that they have no known competing financial interests or personal relationships that could have appeared to influence the work reported in this paper.

Appendix A. Supplementary data

Supplementary data to this article can be found online at https://doi.org/10.1016/j.clae.2025.102447.

References

[1] Papas EB. The global prevalence of dry eye disease: a Bayesian view. *Ophthalmic Physiol Opt* 2021;41(6):1254–66. https://doi.org/10.1111/opo.12888.

[2] Nichols KK, Foulks GN, Bron AJ, et al. The international workshop on meibomian gland dysfunction: executive summary. *Invest Ophthalmol Vis Sci* 2011;52(4): 1922–9. https://doi.org/10.1167/iovs.10-6997a.

[3] Knop E, Knop N, Millar T, Obata H, Sullivan DA. The international workshop on meibomian gland dysfunction: report of the subcommittee on anatomy, physiology, and pathophysiology of the meibomian gland. *Invest Ophthalmol Vis Sci* 2011;52(4): 1938–78. https://doi.org/10.1167/iovs.10-6997c.

[4] Green-Church KB, Butovich I, Willcox M, et al. The international workshop on meibomian gland dysfunction: report of the subcommittee on tear film lipids and lipid-protein interactions in health and disease. *Invest Ophthalmol Vis Sci* 2011;52(4):1979–93. https://doi.org/10.1167/iovs.10-6997d.

[5] Shine WE, McCulley JP. Keratoconjunctivitis sicca associated with meibomian secretion polar lipid abnormality. *Arch Ophthalmol* 1998;116(7):849–52. https://doi.org/10.1001/archopht.116.7.849.

[6] Schaumberg DA, Nichols JJ, Papas EB, Tong L, Uchino M, Nichols KK. The international workshop on meibomian gland dysfunction: report of the subcommittee on the epidemiology of, and associated risk factors for, MGD. *Invest Ophthalmol Vis Sci* 2011;52(4):1994–2005. https://doi.org/10.1167/iovs.10-6997e.

[7] Pult H, Riede-Pult B. Comparison of subjective grading and objective assessment in meibography. *Cont Lens Anterior Eye* 2013;36(1):22–7. https://doi.org/10.1016/j.clae.2012.10.074.

[8] Ban Y, Shimazaki-Den S, Tsubota K, Shimazaki J. Morphological evaluation of meibomian glands using noncontact infrared meibography. *Ocul Surf* 2013;11(1):47–53. https://doi.org/10.1016/j.jtos.2012.09.005.

[9] Adil MY, Xiao J, Olafsson J, et al. Meibomian gland morphology is a sensitive early indicator of meibomian gland dysfunction. *Am J Ophthalmol* 2019;200:16–25. https://doi.org/10.1016/j.ajo.2018.12.006.

[10] Arita R, Itoh K, Maeda S, et al. Meibomian gland duct distortion in patients with perennial allergic conjunctivitis. *Cornea* 2010;29(8):858–60. https://doi.org/10.1097/ICO.0b013e3181ca3668.

[11] Llorens-Quintana C, Rico-Del-Viejo L, Syga P, Madrid-Costa D, Iskander DR. Meibomian gland morphology: the influence of structural variations on gland function and ocular surface parameters. *Cornea* 2019;38(12):1506–12. https://doi.org/10.1097/ICO.0000000000002141.

[12] Dai Q, Liu X, Lin X, et al. A novel meibomian gland morphology analytic system based on a convolutional neural network. *IEEE Access* 2021;9:23083–94. https://doi.org/10.1109/ACCESS.2021.3056234.

[13] Setu MAK, Horstmann J, Schmidt S, Stern ME, Steven P. Deep learning-based automatic meibomian gland segmentation and morphology assessment in infrared meibography. *Sci Rep* 2021;11(1):7649. https://doi.org/10.1038/s41598-021-87314-8.

[14] Rico-Del-Viejo L, Lorente-Velázquez A, Hernández-Verdejo JL, García-Mata R, Benítez-Del-Castillo JM, Madrid-Costa D. The effect of ageing on the ocular surface parameters. *Cont Lens Anterior Eye* 2018;41(1):5–12. https://doi.org/10.1016/j.clae.2017.09.015.

[15] Arita R, Itoh K, Inoue K, Amano S. Noncontact infrared meibography to document age-related changes of the meibomian glands in a normal population. *Ophthalmology* 2008;115(5):911–5. https://doi.org/10.1016/j.ophtha.2007.06.031.

[16] Den S, Shimizu K, Ikeda T, Tsubota K, Shimmura S, Shimazaki J. Association between meibomian gland changes and aging, sex, or tear function. *Cornea* 2006;25(6):651–5. https://doi.org/10.1097/01.ico.0000227889.11500.6f.

[17] Yeotikar NS, Zhu H, Markoulli M, Nichols KK, Naduvilath T, Papas EB. Functional and morphologic changes of meibomian glands in an asymptomatic adult population. *Invest Ophthalmol Vis Sci* 2016;57(10):3996–4007. https://doi.org/10.1167/iovs.15-18467.

[18] Mizoguchi T, Arita R, Fukuoka S, Morishige N. Morphology and function of meibomian glands and other tear film parameters in junior high school students. *Cornea* 2017;36(8):922–6. https://doi.org/10.1097/ICO.0000000000001252.

[19] Gupta PK, Stevens MN, Kashyap N, Priestley Y. Prevalence of meibomian gland atrophy in a pediatric population. *Cornea* 2018;37(4):426–30. https://doi.org/10.1097/ICO.0000000000001476.

[20] Arita R, Itoh K, Maeda S, et al. Proposed diagnostic criteria for obstructive meibomian gland dysfunction. *Ophthalmology* 2009;116(11):2058–2063.e1. https://doi.org/10.1016/j.ophtha.2009.04.037.

[21] Fatima A, Vadla P, Konda N. Changes in the tear film and meibomian gland morphology between preclinical dry eye and normal subjects represented by ocular surface disease index scores. *Exp Eye Res* 2022;222:109188. https://doi.org/10.1016/j.exer.2022.109188.

[22] Arita R, Suehiro J, Haraguchi T, Shirakawa R, Tokoro H, Amano S. Objective image analysis of the meibomian gland area. *Br J Ophthalmol* 2014;98(6):746–55. https://doi.org/10.1136/bjophthalmol-2012-303014.

[23] Gulmez Sevim D, Gumus K, Unlu M. Reliable, noncontact imaging tool for the evaluation of meibomian gland function: sirius meibography. *Eye Contact Lens* 2020;46(Suppl 2):S135–40. https://doi.org/10.1097/ICL.0000000000000651.

[24] Fernández I, Enríquez-De-salamanca A, Portero A, García-Vázquez C, Calonge M, Herreras JM. Age-and sex-adjusted reference intervals in tear cytokine levels in healthy subjects. Appl Sci 2021;11(19):8958. https://doi.org/10.3390/APP11198958.

[25] Chamitava L, Garcia-Larsen V, Cazzoletti L, et al. Determination of adjusted reference intervals of urinary biomarkers of oxidative stress in healthy adults using GAMLSS models. *PLoS One* 2018;13(10). https://doi.org/10.1371/JOURNAL.PONE.0206176.

[26] Tideman JWL, Polling JR, Vingerling JR, et al. Axial length growth and the risk of developing myopia in European children. *Acta Ophthalmol* 2018;96(3):301–9. https://doi.org/10.1111/AOS.13603.

[27] Rigby RA, Stasinopoulos DM, Lane PW. Generalized additive models for location, scale and shape. *J R Stat Soc Ser C Appl Stat* 2005;54(3):507–54. https://doi.org/10.1111/j.1467-9876.2005.00510.x.

[28] Schiffman RM, Christianson MD, Jacobsen G, Hirsch JD, Reis BL. Reliability and validity of the ocular surface disease index. *Arch Ophthalmol* 2000;118(5):615–21. https://doi.org/10.1001/archopht.118.5.615.

[29] Sullivan BD, Whitmer D, Nichols KK, et al. An objective approach to dry eye disease severity. *Invest Ophthalmol Vis Sci* 2010;51(12):6125–30. https://doi.org/10.1167/iovs.10-5390.

[30] Bron AJ, Evans VE, Smith JA. Grading of corneal and conjunctival staining in the context of other dry eye tests. *Cornea* 2003;22(7):640–50. https://doi.org/10.1097/00003226-200310000-00008.

[31] Craig JP, Nichols KK, Akpek EK, et al. TFOS DEWS II definition and classification report. *Ocul Surf* 2017;15(3):276–83. https://doi.org/10.1016/j.jtos.2017.05.008.

[32] Bron AJ, Benjamin L, Snibson GR. Meibomian gland disease. Classification and grading of lid changes. *Eye (Lond)* 1991;5(Pt 4):395–411. https://doi.org/10.1038/eye.1991.65.

[33] Shimazaki J, Goto E, Ono M, Shimmura S, Tsubota K. Meibomian gland dysfunction in patients with Sjögren syndrome. *Ophthalmology* 1998;105(8):1485–8. https://doi.org/10.1016/S0161-6420(98)98033-2.

[34] Tesón M, González-García MJ, López-Miguel A, et al. Influence of a controlled environment simulating an in-flight airplane cabin on dry eye disease. *Invest Ophthalmol Vis Sci* 2013;54(3):2093–9. https://doi.org/10.1167/iovs.12-11361.

[35] Yamaguchi M, Kutsuna M, Uno T, Zheng X, Kodama T, Ohashi Y. Marx line: fluorescein staining line on the inner lid as indicator of meibomian gland function. *Am J Ophthalmol* 2006;141(4):669–75. https://doi.org/10.1016/j.ajo.2005.11.004.

[36] Bunn A, Korpela M. R: A language and environment for statistical computing. Published online 2013. doi:10.1016/j.dendro.2008.01.002.

[37] Dunn PK, Smyth GK. Randomized Quantile Residuals. *J Comput Graph Stat* 1996;5(3):236–44. https://doi.org/10.1080/10618600.1996.10474708.

[38] Llorens-Quintana C, Rico-Del-Viejo L, Syga P, Madrid-Costa D, Iskander DR. A novel automated approach for infrared-based assessment of meibomian gland morphology. *Transl Vis Sci Technol* 2019;8(4):17. https://doi.org/10.1167/tvst.8.4.17.

[39] Xiao P, Luo Z, Deng Y, Wang G, Yuan J. An automated and multiparametric algorithm for objective analysis of meibography images. *Quant Imaging Med Surg* 2021;11(4):1586–99. https://doi.org/10.21037/qims-20-611.

[40] Chen X, Badian RA, Hynne H, et al. Morphology of meibomian glands in a 65-year-old Norwegian population without dry eye disease. *J Clin Med* 2022;11(3):527. https://doi.org/10.3390/jcm11030527.

[41] Eom Y, Choi KE, Kang SY, Lee HK, Kim HM, Song JS. Comparison of meibomian gland loss and expressed meibum grade between the upper and lower eyelids in patients with obstructive meibomian gland dysfunction. *Cornea* 2014;33(5):448–52. https://doi.org/10.1097/ICO.0000000000000092.

[42] Nelson JD, Shimazaki J, Benitez-del-Castillo JM, et al. The international workshop on meibomian gland dysfunction: report of the definition and classification subcommittee. *Invest Ophthalmol Vis Sci* 2011;52(4):1930–7. https://doi.org/10.1167/iovs.10-6997b.

[43] Bron AJ, Tiffany JM. The contribution of meibomian disease to dry eye. *Ocul Surf* 2004;2(2):149–65. https://doi.org/10.1016/s1542-0124(12)70150-7.

[44] Finis D, Ackermann P, Pischel N, et al. Evaluation of Meibomian gland dysfunction and local distribution of meibomian gland atrophy by non-contact infrared meibography. *Curr Eye Res* 2015;40(10):982–9. https://doi.org/10.3109/02713683.2014.971929.

[45] Butovich IA, Lu H, McMahon A, et al. Biophysical and morphological evaluation of human normal and dry eye meibum using hot stage polarized light microscopy. *Invest Ophthalmol Vis Sci* 2014;55(1):87–101. https://doi.org/10.1167/iovs.13-13355.

[46] Borchman D, Foulks GN, Yappert MC, et al. Human meibum lipid conformation and thermodynamic changes with meibomian-gland dysfunction. *Invest Ophthalmol Vis Sci* 2011;52(6):3805–17. https://doi.org/10.1167/iovs.10-6514.

[47] Straatsma BR. Cystic degeneration of the meibomian glands. *AMA Arch Ophthalmol* 1959;61(6):918–27. https://doi.org/10.1001/archopht.1959.00940090920007.

[48] Gutgesell VJ, Stern GA, Hood CI. Histopathology of meibomian gland dysfunction. *Am J Ophthalmol* 1982;94(3):383–7. https://doi.org/10.1016/0002-9394(82)90365-8.

[49] Xiao J, Adil MY, Olafsson J, et al. Diagnostic test efficacy of meibomian gland morphology and function. *Sci Rep* 2019;9(1):17345. https://doi.org/10.1038/s41598-019-54013-4.

[50] Tomlinson A, Bron AJ, Korb DR, et al. The international workshop on meibomian gland dysfunction: report of the diagnosis subcommittee. *Invest Ophthalmol Vis Sci* 2011;52(4):2006–49. https://doi.org/10.1167/IOVS.10-6997F.

[51] Deng Y, Wang Q, Luo Z, et al. Quantitative analysis of morphological and functional features in meibography for meibomian gland dysfunction: diagnosis and grading. *EClinicalMedicine* 2021;40:101132. https://doi.org/10.1016/j.eclinm.2021.101132.

[52] Wolffsohn JS, Arita R, Chalmers R, et al. TFOS DEWS II diagnostic methodology report. *Ocul Surf* 2017;15(3):539–74. https://doi.org/10.1016/j.jtos.2017.05.001.

[53] Pucker AD, Jones-Jordan LA, Kunnen CME, et al. Impact of meibomian gland width on successful contact lens use. *Cont Lens Anterior Eye* 2019;42(6):646–51. https://doi.org/10.1016/j.clae.2019.06.004.

[54] Swiderska K, Blackie CA, Maldonado-Codina C, Fergie M, Read ML, Morgan PB. Evaluation of Meibomian gland structure and appearance after therapeutic Meibomian gland expression. *Clin Exp Optom* 2024;107(5):504–14. https://doi.org/10.1080/08164622.2023.2251994.

[55] Swiderska K, Blackie CA, Maldonado-Codina C, Fergie M, Read ML, Morgan PB. Temporal variations in meibomian gland structure-a pilot study. *Ophthalmic Physiol Opt* 2024;44(5):894–909. https://doi.org/10.1111/opo.13321.